Journal of Photochemistry and Photobiology A: Chemistry 208 (2009) 13–20

Contents lists available at ScienceDirect

Journal of Photochemistry and Photobiology A: Chemistry

journal homepage: www.elsevier.com/locate/jphotochem

Effect of substituents on the photoluminescence performance of Ir(III) complexes: Synthesis, electrochemistry and photophysical properties

J. Jayabharathi[a,*], V. Thanikachalam[b], K. Saravanan[a]

[a] Department of Chemistry, Annamalai University, Annamalainagar 608 002, India
[b] Department of Chemistry (DDE), Annamalai University, Annamalainagar 608 002, India

ARTICLE INFO

Article history:
Received 4 April 2009
Received in revised form 24 July 2009
Accepted 29 July 2009
Available online 5 August 2009

Keywords:
Imidazole ligand
Iridium complex
Absorption spectrum
Emission spectrum
Cyclic voltammetry

ABSTRACT

We have prepared and characterized a series of substituted imidazole ligands namely dmmppi, dmmpfpi, dmdmppi and dmdmpfpi. These compounds will readily undergo cyclometalation with iridium trichloride and form di-irrido and the six coordinated iridium(III) dopants of the substituted imidazole ligands. They emit green colour both in solid and in solution phase. The peak emission wavelength of the dopants (λ_{max} = 428–497 nm) can be finely tuned depending upon the electronic properties of the phenyl, fluorophyenyl, methoxy phenyl and dimethoxyphenyl substituents as well as their positions in the imidazole ring. These iridium complexes namely Ir(dmmppi)$_2$(pic) **1a**, Ir(dmmpfpi)$_2$(pic) **1b**, Ir(dmdmppi)$_2$(pic) **1c** and Ir(dmdmpfpi)$_2$(pic) **1d** were characterized by ^{1}H NMR, MS and elemental analysis. All these iridium complexes **1a**–**1d** show unusual high HOMO levels (E_{HOMO} = 5.21–5.41 eV) and high phosphorescence. These complexes emit green light with exceedingly high efficiency.

1. Introduction

Organic electroluminescent materials have attracted considerable interest among academic and industrial communities since the seminal reports on molecular and polymeric organic light-emitting diodes (OLEDs) by Tang et al. [1] and Burroughes et al. [2] respectively. In most OLEDs, triplet states constitute 75% of electrogenerated excited states. These triplet states are generally non-emissive due to their long lifetime (commonly from milliseconds to minutes) as well as their spin-forbidden nature for radiative relaxation to the ground states. Consequently, the maximum internal quantum efficiency of OLEDs is normally limited to 25%. To remove such constraint, efforts have been directed in using transition metal complexes, particularly 4d and 5d metals [3–5]. The strong spin–orbit coupling caused by heavy metal ions in these complexes results in efficient intersystem crossing from the singlet to the triplet excited state. Mixing of the singlet and triplet excited states not only removes the spin-forbidden nature of the radiative relaxation of the triplet state but also significantly shortens the triplet state lifetime. Triplet–triplet annihilation is more effectively suppressed because of the shorter lifetime of the triplet excited state. Therefore, higher phosphorescence efficiencies can be achieved.

Numerous organometallic d^6, d^8 and d^{10} complexes are luminescent in solution or solid state [6–23]. Among these Os(II) [13], Cu(I) [14], cyclometalated Ir(III) [15–20] and Pt(II) complexes [21–23] have been fabricated into light-emitting devices. Cyclometalated iridium(III) complexes receive the most extensive study partly due to their ease of preparation from iridium precursors with the corresponding imines which are capable of undergoing cyclometalation [24]. Most of the iridium complexes used in these studies consist of cyclometalated imidazole derivatives as ligands.

Synthesis [25] and photophysical properties of some substituted imidazole based Ir(III) complexes were also reported [19,26,27]. In this paper, we report the synthesis, electrochemical and photophysical properties of the iridium complexes. These complexes show unusual high HOMO levels and exhibit exceedingly high efficiency even at relatively low dopant concentration.

2. Experimental

2.1. Materials and methods

All of the preparative work involving iridium(III) trichloride hydrate ($IrCl_3{\cdot}3H_2O$, Sigma–Aldrich Ltd.), 2-ethoxyethanol ($H_5C_2OC_2H_4OH$, S.D. Fine) and all other reagents were carried out in an inert atmosphere and used without further purification.

2.2. Optical measurements and compositions analysis

The ultraviolet–visible (UV–vis) spectra of the phosphorescent Ir(III) complexes were measured on an UV–vis spectrophotometer (UV-1650 PC SHIMADZU) and corrected for background due to

* Corresponding author. Tel.: +91 4144 239523.
E-mail address: jtchalam2005@yahoo.co.in (J. Jayabharathi).

1010-6030/$ – see front matter © 2009 Elsevier B.V. All rights reserved.
doi:10.1016/j.jphotochem.2009.07.027

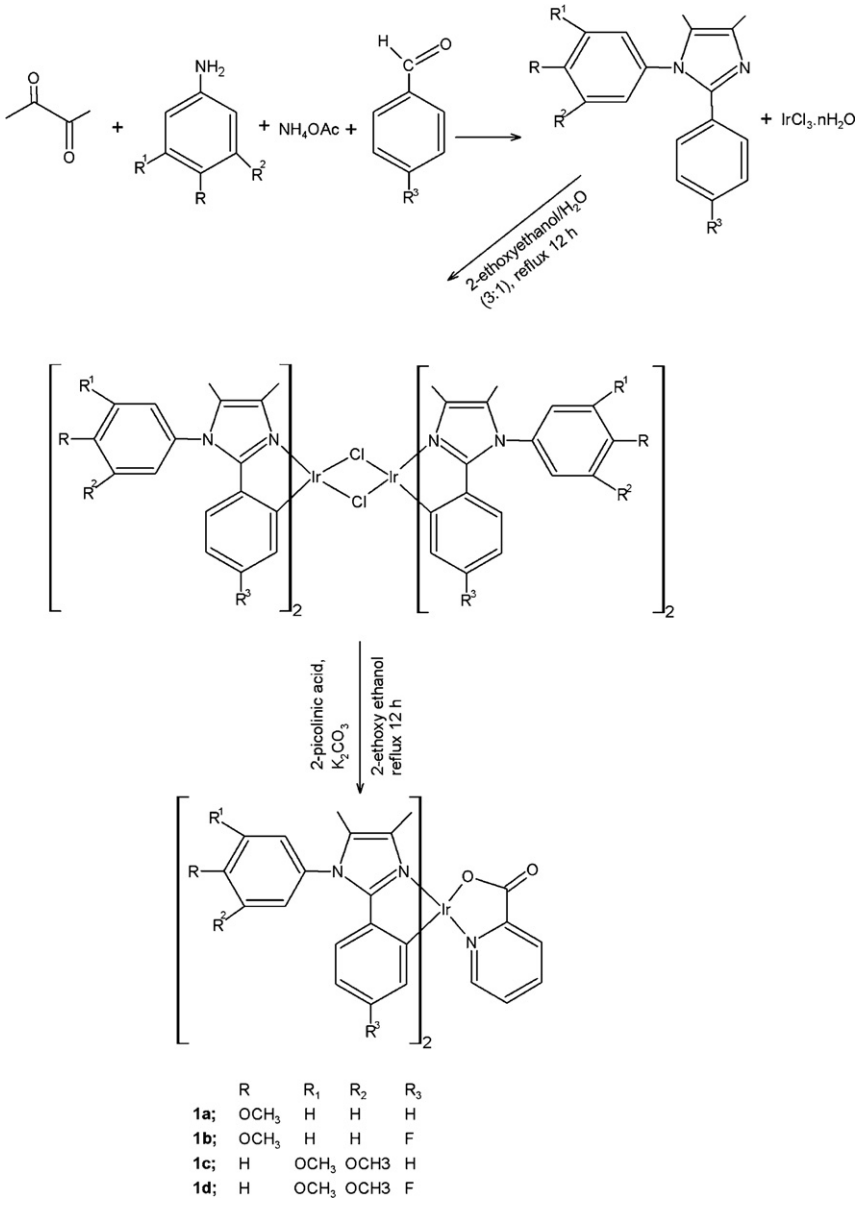

	R	R_1	R_2	R_3
1a;	OCH_3	H	H	H
1b;	OCH_3	H	H	F
1c;	H	OCH_3	OCH3	H
1d;	H	OCH_3	OCH3	F

Scheme 1. Synthesis of ligands and iridium complexes $(C\hat{N})_2Ir(pic)$ **1a**–**1d**.

solvent absorption. Photoluminescence (PL) spectra were recorded on a (Perkin Elmer LS55) fluorescence spectrometer. The solid-state emission spectra were recorded on fluoromax 2 (ISA SPEX) xenon-Arc lamp as a source. NMR spectra were recorded on Bruker 400 MHz. MS spectra (EI and FAB) were carried out by using a Varian Saturn 2200. Cyclic voltammetry (CV) analysis was performed by using CHI 630A potentiostap electrochemical analyzer.

2.3. General procedure for the synthesis of ligands

The various substituted imidazole ligands were prepared from an unusual four components assembling of 1,2-dione, ammonia, arylamine and an arylaldehyde as shown in Scheme 1 [28].

2.3.1. 4,5-Dimethyl-1-(4′-methoxyphenyl)-2-phenyl-1H-imidazole (dmmppi)

Yield: 50%. Anal. calcd. for $C_{18}H_{18}N_2O$: C, 77.67; H, 6.52; N, 10.06. Found: C, 77.14; H, 6.32; N, 9.87. ^{1}H NMR (400 MHz, $CDCl_3$): δ 2.29 (s, 3H), 2.02 (s, 3H), 3.85 (s, 3H), 6.91–7.10 (aromatic protons). MS: m/z 278.2, calcd. 278.36.

2.3.2. 4,5-Dimethyl-1-(4′-methoxyphenyl)-2-(p-fluorophenyl)-1H-imidazole (dmmpfpi)

Yield: 40%. Anal. calcd. for $C_{18}H_{17}N_2OF$: C, 72.95; H, 5.78; N, 9.45. Found: C, 72.24; H, 5.36; N, 8.98. ^{1}H NMR (400 MHz, $CDCl_3$): δ 2.28 (s, 3H), 1.99 (s, 3H), 3.85 (s, 3H), 6.85–7.35 (aromatic protons). MS: m/z 296.5, calcd. 296.35.

2.3.3. 4,5-Dimethyl-1-(3′5′-dimethoxyphenyl)-2-phenyl-1H-imidazole (dmdmppi)

Yield: 45%. Anal. calcd. for $C_{19}H_{20}N_2O_2$: C, 73.93; H, 6.54; N, 9.08. Found: C, 73.23; H, 6.18; N, 8.79. ^{1}H NMR (400 MHz, $CDCl_3$): δ 2.29 (s, 3H), 2.05 (s, 3H), 3.73 (s, 6H), 6.32–7.43 (aromatic protons). MS: m/z 308.3, calcd. 308.38.

2.3.4. 4,5-Dimethyl-1-(3′,5′-dimethoxyphenyl)-2-(p-fluorophenyl)-1H-imidazole (dmdmpfpi)

Yield: 45%. Anal. calcd. for $C_{19}H_{19}N_2O_2F$: C, 69.92; H, 5.87; N, 8.58. Found: C, 69.12; H, 5.37; N, 8.24. ^{1}H NMR (400 MHz, $CDCl_3$): δ 2.28 (s, 3H), 2.04 (s, 3H), 3.74 (s, 6H), 6.30–7.40 (aromatic protons). MS: m/z 326.3, calcd. 326.37.

*2.4. General procedure for the synthesis of iridium complexes (**1a**–**1d**)*

The imidazole based cyclometalated iridium complexes **1a**–**d** were readily synthesized from $IrCl_3 \cdot nH_2O$ and the imidazole ligands to give the corresponding dimeric species via the Nonoyama route [29] followed by the treatment with 2-picolinic acid in the presence of K_2CO_3 as shown in Scheme 1.

2.4.1. Iridium(III)bis(4,5-dimethyl-(4′-methoxyphenyl)-2-phenyl-1H-imidazolato-N,C$^{2'}$)(picolinate) (Ir(dmmppi)$_2$(pic)), ***1a***

Yield: 62%. Anal. calcd. for $C_{42}H_{38}IrN_5O_4$: C, 58.05; H, 4.41; N, 8.06. Found: C, 57.98; H, 4.36; N, 8.03. ^{1}H NMR (400 MHz, $CDCl_3$): δ 8.58 (d, J = 5.0 Hz, 1H), 7.88 (dd, J = 6.0, 9.0 Hz, 2H), 7.59 (d, J = 7.5 Hz, 1H), 7.34 (dd, J = 5.5 Hz, 9.0 2H), 6.03 (d, J = 2.0 Hz, 1H), 7.14 (t, J = 8.0 Hz, 2H), 6.87 (t, J = 9.0 Hz, 2H), 6.49 (m, 2H), 6.27 (m, 2H), 7.05 (s, 1H), 3.89 (s, 6H), 2.05 (s, 6H), 1.92 (s, 6H). MS: m/z 868.6, calcd. 869.0.

2.4.2. Iridium(III)bis(4,5-dimethyl-1-(4′-methoxyphenyl)-2-(p-fluorophenyl)-1H-imidazolato-N,C$^{2'}$)(picolinate) (Ir(dmmpfpi)$_2$(pic)), ***1b***

Yield: 78%. Anal. calcd. for $C_{42}H_{36}F_2IrN_5O_4$: C, 55.74; H, 4.01, N, 7.74. Found: C, 55.34; H, 3.02; N, 7.36. ^{1}H NMR (400 MHz, $CDCl_3$): δ 8.25 (d, 1H), 7.82 (t, J = 9.5 Hz, 1H), 7.84 (d, J = 6.5 Hz, 1H), 7.20 (dd, J = 4.0 Hz, 2H), 7.32 (dd, J = 3.0, 11.0 Hz, 2H), 7.05 (m, 1H), 7.02 (dd, J = 3.5, 7.0 Hz, 2H), 6.09 (dd, J = 3.0 Hz, 13 Hz, 2H), 3.89 (s, 6H), 1.82 (s, 6H), 1.28 (s, 6H). MS: m/z 904.6, calcd. 904.98.

2.4.3. Iridium(III)bis(4,5-dimethyl-1-(3′,5′-dimethoxyphenyl)-2-phenyl-1H-imidazolato-N,C$^{2'}$)(picolinate) (Ir(dmdmppi)$_2$(pic)), ***1c***

Yield: 72%. Anal. calcd. for $C_{44}H_{42}IrN_5O_6$: C, 56.88; H, 4.56; N, 7.54. Found: C, 56.01; H, 4.26; N, 7.01. ^{1}H NMR (400 MHz, $CDCl_3$): δ 8.27 (d, J = 7.2 Hz, 1H), 7.85 (d, J = 5.4 Hz, 1H), 7.81 (dd, J = 1.6 Hz, 1H), 7.32 (m, 1H), 6.64 (t, J = 3.52 Hz, 2H), 6.68 (m, 1H), 6.55 (m, 1H), 6.34 (d, J = 2.10 Hz, 4H), 3.76 (s, 12H), 2.07 (s, 6H), 1.97 (s, 6H). MS: m/z 928.6, calcd. 929.05.

2.4.4. Iridium(III)bis(4,5-dimethyl-1-(3′,5′-dimethoxyphenyl)-2-(p-fluorophenyl)-1H-imidazolato-N,C$^{2'}$)(picolinate) (Ir(dmdmpfpi)$_2$(pic)), ***1d***

Yield: 67%. Anal. calcd. for $C_{44}H_{40}F_2IrN_5O_6$: C, 54.76; H, 4.18; N, 7.26. Found: C, 54.37; H, 4.03; N, 7.13. ^{1}H NMR (400 MHz, $CDCl_3$): δ 7.86 (m, 1H), 7.32 (m, 1H), 6.65 (dd, 1H), 6.39 (dd, 1H), 7.74 (m, 2H), 7.07 (t, 4H), 6.63 (t, 2H), 6.33 (d, 4H), 3.79 (s, 12H), 2.56 (s, 6H), 2.08 (s, 6H). MS: m/z 964.6, calcd. 965.03.

3. Results and discussion

3.1. Synthesis and characterization of (CN̂)$_2$Ir(pic) complexes

The synthetic method used to prepare these complexes involves two steps. In the first step, $IrCl_3 \cdot 3H_2O$ was allowed to react with an excess of the cyclometalated ligand (2–5 times) to give a chloride-bridged dinuclear complex, i.e., $(C\hat{N})_2Ir(\mu\text{-}Cl)_2(C\hat{N})_2$. The NMR spectra of these complexes are in consistent with the heterocyclic ring, i.e., imidazole ring being in a *trans* position. The chloride-bridged dinuclear complexes can be readily converted to emissive, mononuclear complexes $(C\hat{N})_2Ir(pic)$ by replacing the two bridging chlorides with bidentate 2-picolinic acid. These reactions result in $(C\hat{N})_2Ir(pic)$ with a yield of 62–78%.

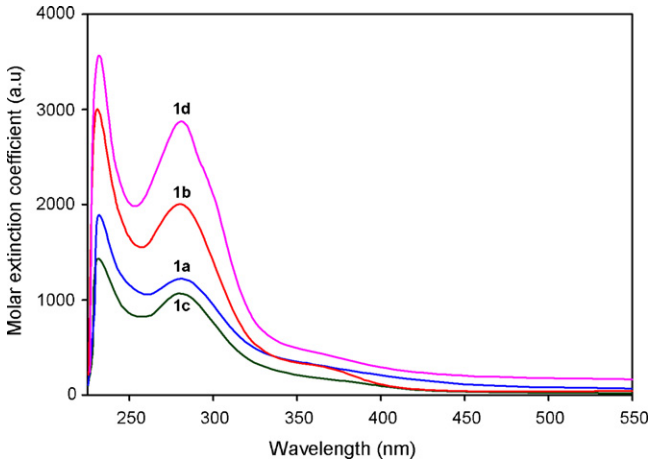

Fig. 1. The UV–vis absorption spectra of the complexes **1a**–**1d** in CH_2Cl_2.

The iridium(III) ion is octahedrally coordinated by the three chelating ligands. The coordination geometry of the $(C\hat{N})_2Ir(pic)$ fragment in the mononuclear complex is the same as that for the dinuclear complexes. The mononuclear complexes can be sublimed easily at reduced pressure. ^{1}H NMR data for the ligands and mononuclear complexes fall in the range of 8.58–1.27 ppm, respectively.

3.2. Absorption spectra

Fig. 1 shows the absorption bands of **1a**–**1d** as representative of the series of complexes. It suggests that the bands can be classified into two types. The intense bands observed around 230 nm in the ultraviolet part of the spectrum can be assigned to the allowed ligand centered (π–π^*) transitions [24] somewhat weaker bands are observed in the lower part of energy (λ_{max} > 360 nm). The band position, size and the extinction coefficients suggest that these are MLCT transitions [24,30]. ^{1}MLCT and ^{3}MLCT transitions have been resolved in the range of 270–400 nm as indicated in Table 1. Absorption in the range of around 270–400 nm for all the complexes corresponds to the transition of the ^{1}MLCT state as evident from its extinction coefficient of the order 10^3. The absorption like long tail toward lower energy and higher wavelength around 360 is assigned to ^{3}MLCT transitions and gains intensity by mixing with the higher lying ^{1}MLCT transitions through the spin–orbit coupling of iridium(III) [30]. This mixing is strong enough in these complexes that are formally spin forbidden. ^{3}MLCT has an extinction coefficient that is almost equal to the spin allowed transition. The key photophysical data are summarized in Table 1.

3.3. Quantum efficiency and lifetime

The PL quantum yields measured in dichloromethane, using coumarin 47 in ethanol as a standard [31] for complexes **1a**–**1d** are 0.30, 0.15, 0.64 and 0.36, respectively according to Eq. (1)

$$\phi_{unk} = \phi_{std}\left(\frac{I_{unk}}{I_{std}}\right)\left(\frac{A_{std}}{A_{unk}}\right)\left(\frac{\eta_{unk}}{\eta_{std}}\right)^2 \quad (1)$$

where ϕ_{unk}, ϕ_{std}, I_{unk}, I_{std}, A_{unk}, ϕ_{unk} and η_{std} are the fluorescent quantum yields, the integration of the emission intensities, the absorbances at the excitation wavelength, and the refractive

Table 1
Photophysical properties of iridium complexes **1a**–**1d**.

Complex	Absorption[a] (λ, nm) (log ε)	Emission[b] (λ, nm)	HOMO	LUMO[c]	ΔE (eV)	Lifetime (μs)	Quantum yield
$Ir(dmmppi)_2(pic)$, **1a**	232.0 (3.276) 279.0 (3.090) 359.0 (2.505)	433	5.31	1.91	3.40	1.63	0.20
$Ir(dmmpfpi)_2(pic)$, **1b**	230.0 (3.477) 280.5 (3.301) 361 (2.230)	428	5.41	1.96	3.45	1.23	0.15
$Ir(dmdmppi)_2(pic)$, **1c**	231.0 (3.155) 280.0 (3.025) 359.0 (2.230)	497	5.31	2.08	3.23	1.00	0.64
$Ir(dmdmpfpi)_2(pic)$, **1d**	231.0 (3.555) 280.0 (3.456) 360.0 (2.653)	452	5.21	1.83	3.38	1.01	0.36

[a] UV–vis absorption measured in CH_2Cl_2 solution, concentration = 1×10^{-5} M.
[b] Photoluminescence measured in CH_2Cl_2 solution, concentration = 1×10^{-4} M.
[c] Measurement was carried out in CH_2Cl_2 solution, concentration = 1×10^{-3} M.

indexes of the corresponding solutions for the samples and the standard, respectively.

The quantum yield for complexes **1a, 1c** and **1d** are closer to the value of 0.40 for $Ir(PPy)_3$. The photoluminescent lifetime for all these complexes were measured and these values are comparable to that of $Ir(PPy)_3$ and strongly support that complexes **1a**–**1d** are the highly phosphorescent emitters. The relationship between quantum yield and emission peak wavelength of all complexes **1a**–**1d** are shown in graph (Fig. 2a).

The phosphorescence lifetime τ was measured for these complexes **1a**–**1d** in degassed CH_2Cl_2 solutions at room temperature (Fig. 3). The radiative and non-radiative rate constants k_r and k_{nr} were calculated from the phosphorescence yield ϕ_p, and the phosphorescence lifetime τ using the following equation:

$$\phi_p = \phi_{ISC}\{k_r/(k_r + k_{nr})\} \quad (2)$$

ϕ_{ISC} is the intersystem crossing. For iridium complexes ϕ_{ISC} is safely assumed to be 1.0 because of the strong spin–orbit interaction caused by heavy atom effects of iridium.

$$k_r = \frac{\phi_p}{\tau} \quad (3)$$

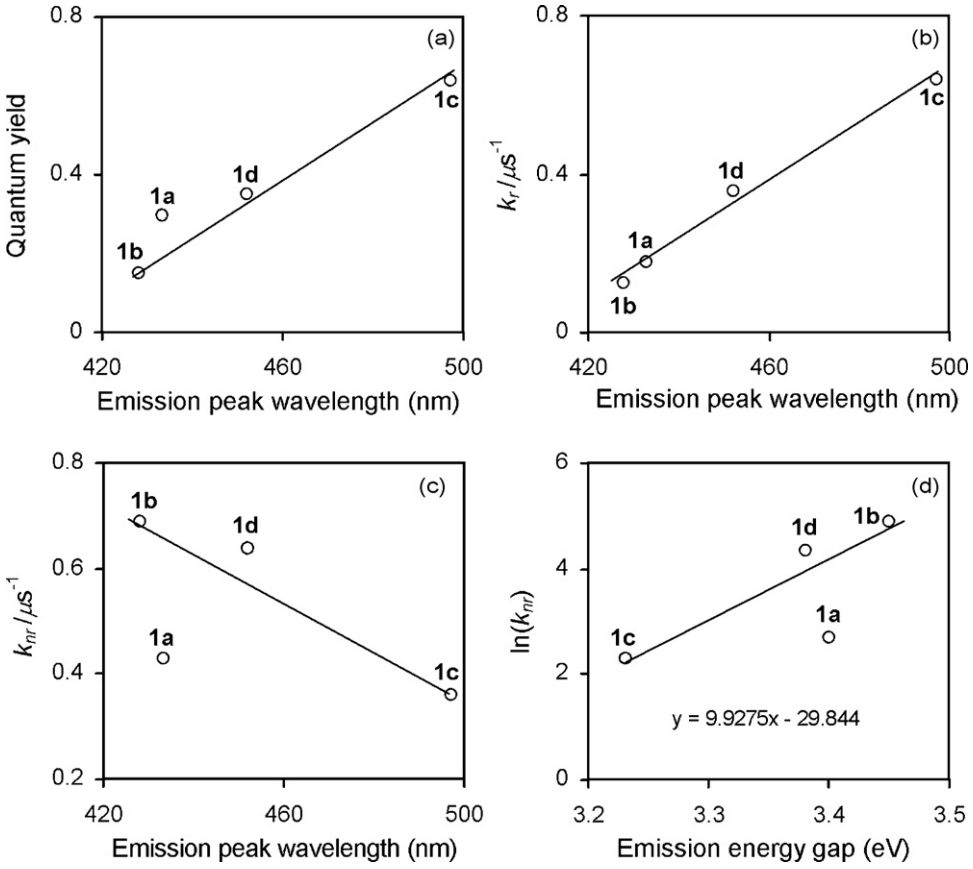

Fig. 2. Quantum yield and decay rate constants of the complexes: (a) quantum yield *versus* emission on peak wavelength; (b) radiative decay rate constant *versus* emission peak wavelength; (c) non-radiative decay rate constant *versus* emission peak wavelength; (d) plot of ln(k_{nr}) *versus* emission energy gap.

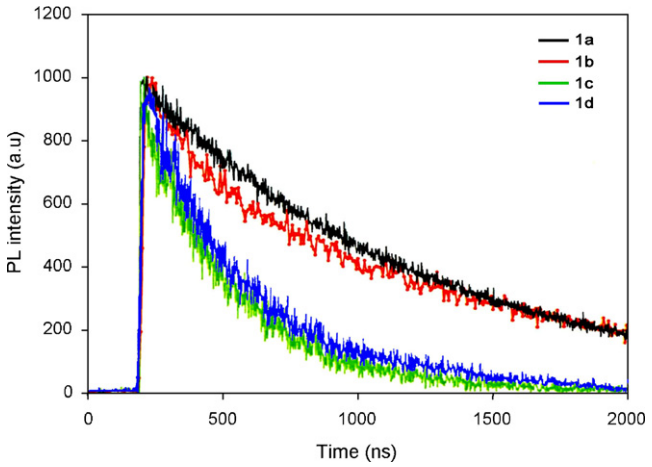

Fig. 3. The lifetime spectra of the complexes **1a**–**1d** in CH_2Cl_2.

$$k_{nr} = \frac{1}{\tau} - \frac{\phi_p}{\tau} \quad (4)$$

Thus, the non-radiative rate constant is a sum of rates for several processes that quench emission. One of these processes could involve bond dissociation in the excited state. Among all the complexes **1a** have a high quantum yield and shows comparably higher radiative constants and smaller non-radiative rate constant. Complex **1b** with lowest quantum yield and high non-radiative rate constant implies that the non-radiative decay of these complexes was several folds faster than radiative decay.

Table 2
Cyclic voltammetry data, radiative and non-radiative constants of **1a**–**1d**.

Complex	k_r (μs^{-1})	k_{nr} (μs^{-1})	$E^{oxi}_{1/2}$
$Ir(dmmppi)_2(pic)$, **1a**	0.18	0.43	0.51
$Ir(dmmpfpi)_2(pic)$, **1b**	0.12	0.69	0.61
$Ir(dmdmppi)_2(pic)$, **1c**	0.64	0.36	0.51
$Ir(dmdmpfpi)_2(pic)$, **1d**	0.36	0.64	0.41

From the view point of the relationship between maximum emission peak wavelength of photoluminescent spectrum and decay rate constant in Table 2 (Fig. 2b and c) two trends are evident for the iridium complexes **1a**–**1d**. The radiative decay rate constant (k_r) increases for the complex **1c** which has the maximum emission peak shift. Additionally the non-radiative rate constants (k_{nr}) does not show monotonous by the maximum emission shift [32]. The plot $\ln(k_{nr})$ *versus* the energy gap (ΔE, eV) for complexes **1a**–**1d** are given in Fig. 2d. The non-radiative rate constant (k_{nr}) values for the fluoro substituted iridium complexes (**1b** and **1d**) are higher than non-fluoro iridium complexes (**1a** and **1c**). The energy gap law predicts that the rate of non-radiative decay increase when the energy gap separating the ground and excited state decreases. The rela-

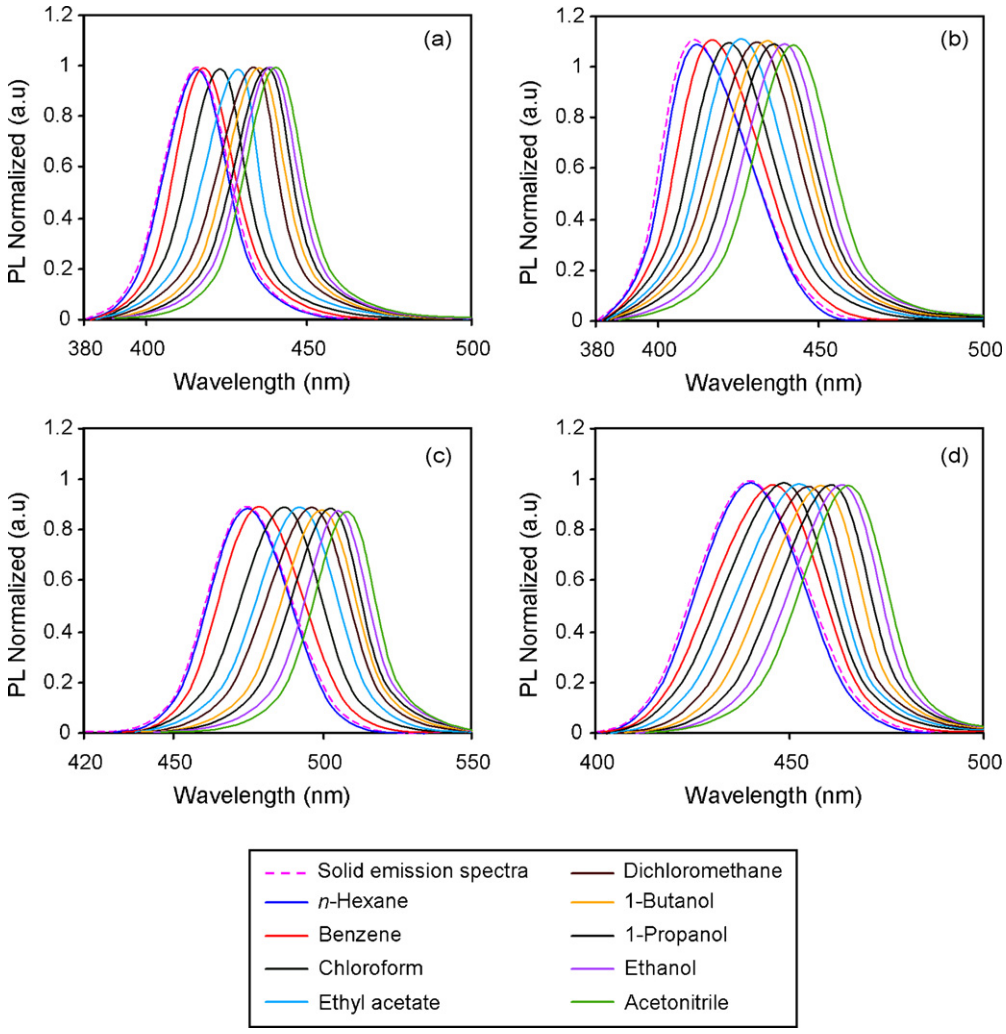

Fig. 4. The solid state and the solvatochromic emission spectra of the complexes **1a**–**1d**.

tion is based on the vibrational overlap between the ground state and the excited state, and k_{nr} is a function of a Franck–Condon overlap integral. In the case of complexes having similar excited states and vibrational coupling, a simplified form of the energy gap law is obtained that predicts a linear relation between $\ln(k_{nr})$ and the energy gap [23]. This correlation suggests that the change of non-radiative decay rate constant is owing to the energy gap of the complexes. The presence of 3′,5′-dimethoxyphenyl group on the imidazole moiety lead to red shift of the emission. Thus, the wavelength of the emission maxima for these four complexes follows the order **1c** > **1d** > **1a** > **1b**.

3.4. Ligand tuning of emission wavelength

All of these complexes (**1a**–**1d**) show strong luminescence both in the solid state (Fig. 4) and in organic solutions (Fig. 5) from their triplet state [24]. The maximum emission peak was found to be dependent on the polarity of the solvent which suggests the MLCT character of the emissions state. The presence of vibrational progression in the PL spectra and significant stokes shift assist us in assigning the $^3(\pi-\pi^*)$ states as the dominant emitting state at room temperature in equilibrium with the other neighbouring states [33]. Typically on changing the substituents, we have observed a marked effect on systematic shifting of the maximum emission peak of iridium complexes as indicated by the solution photoluminescent spectra represented in Fig. 4 as summarized in Table 1. Comparison of the emission wavelength of the complexes **1a**–**1d** shows that complexes containing dimethoxy substituents **1c** and **1d** shows longer emission shift than **1a** and **1b**. It may be due to the electronic nature of the substituents [33].

3.5. Solvatochromism of the complexes *1a*–*1d*

The absorption peaks of the complexes **1a**–**1d** in different solvents are almost the same. This suggests that the polarity of the solvent has very little influence on the energy levels of **1a**–**1d** ground state molecules in Table 3. However the emission peaks of the complexes **1a**–**1d** in different solvents show clear differences in Fig. 4. This emission of complexes **1a**–**1d** peaks at around 420 nm in *n*-hexane (non-polar) 440 nm in ethanol (polar protic solvent) and 435 nm in CH_2Cl_2 (medium polarity) and 480 nm CH_3CN (a strongly polar a protoic solvent). The peak shift can be attributed to the stronger interaction between the solvents and the excited molecules. The excited state of all iridium complexes are more stabilized in polar solvents than in non-polar solvents. This leads to a red shift of emission with increasing solvent polarity [34]. The photoluminescent peaks of solid state of all complexes are close to that of emission in non-polar solvent *n*-hexane. This means that there is little or no influence of molecular interaction on the excited state of iridium complexes in the solid state [34].

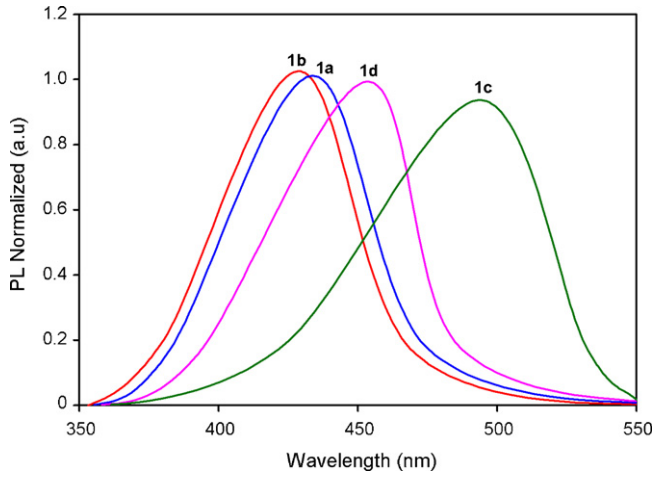

Fig. 5. The photoluminescence emission spectra of the complexes **1a**–**1d** in CH_2Cl_2.

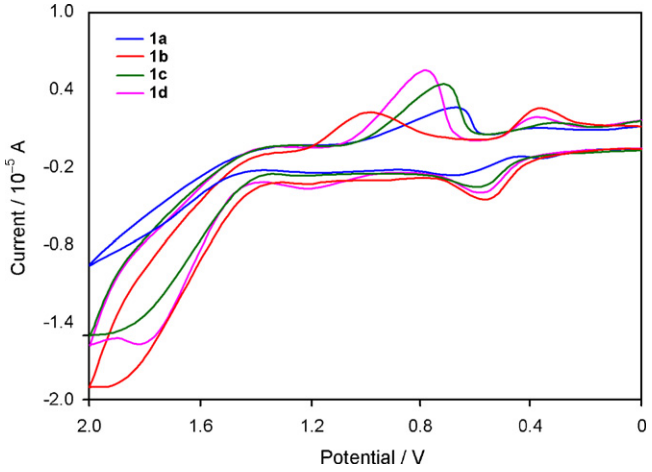

Fig. 6. Cyclic voltammetry of the complexes **1a**–**1d** in CH_2Cl_2.

3.6. Redox chemistry

The electrochemical properties of these complexes were examined by cyclic voltammetry (Fig. 6). The redox potential was measured relative to an internal ferrocene reference ($Cp_2Fe/Cp_2Fe^+ = 0.45$ V *versus* SCE in CH_2Cl_2 solvent). The HOMO/LUMO [35] energy has been calculated for all the complexes based on the experimental redox potential value and the lowest energy absorbance edges of the UV–visible absorption–emission spectra wavelength (0–0) onset point. The energy level of the highest occupied molecular orbital (HOMO) and lowest unoccupied molecular orbital (LUMO) is calculated using the following Eqs. (5) and (6):

$$E_{HOMO} = E^{oxi}_{1/2} + 4.8 \quad (5)$$

$$E_{LUMO} = E_{HOMO} - E_g \quad (6)$$

where $E^{oxi}_{1/2}$ = oxidation potential of complexes; $E_g = \frac{hc}{\lambda}/(0-0)$ onset point and 4.8 eV energy level of the ferrocene.

These iridium complexes show reversible oxidation behavior with lower oxidation potentials relative to the pyridine based iridium complexes. As a result, these complexes exhibit exceedingly

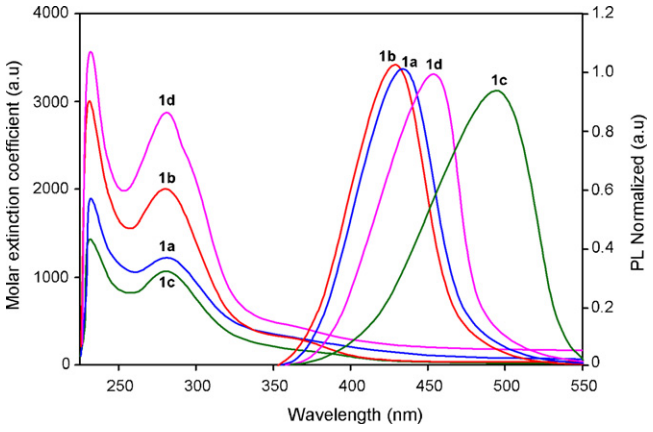

Fig. 7. Normalized UV–vis absorption and photoluminescence spectra of complexes **1a**–**1d** in CH_2Cl_2.

Table 3
Photoluminescence spectral data at various solvents and solid emission spectra of complexes **1a**–**1d**.

Solvents	Absorption[a] (λ, nm) (log ε)				Emission[b] (λ, nm)			
	1a	**1b**	**1c**	**1d**	**1a**	**1b**	**1c**	**1d**
n-Hexane	230.0 (3.152) 276.0 (3.028) 358.0 (2.402)	231.0 (3.262) 278.0 (2.992) 359.0 (2.186)	230.0 (3.098) 279.0 (3.080) 359.0 (2.178)	229.0 (3.520) 279.0 (3.362) 358.0 (2.540)	415.0	408.0	475.0	437.0
Benzene	230.0 (3.180) 276.0 (3.033) 357.7 (2.308)	230.0 (3.466) 278.0 (2.986) 359.0 (2.165)	231.0 (3.106) 278.0 (3.026) 359.0 (2.162)	228.0 (3.486) 280.0 (3.368) 359.5 (2.538)	417.0	412.0	478.0	442.0
Chloroform	231.5 (3.105) 277.0 (3.198) 358.0 (2.502)	230.5 (3.292) 279.0 (2.802) 361.0 (2.158)	230.0 (3.112) 279.0 (3.030) 358.0 (2.172)	230.0 (3.492) 278.0 (3.408) 358.0 (2.610)	422.0	417.0	485.0	444.0
Ethyl acetate	230.5 (3.207) 278.0 (3.056) 359.0 (2.507)	232.0 (3.398) 277.0 (2.906) 361.0 (2.168)	229.5 (3.148) 280.0 (3.019) 359.0 (2.206)	231.0 (3.498) 280.0 (3.462) 359.0 (2.635)	427.0	423.0	492.0	450.0
Dichloromethane	232.0 (3.276) 279.0 (3.090) 359.0 (2.505)	230.0 (3.477) 280.5 (3.301) 361.0 (2.230)	231.0 (3.155) 280.0 (3.025) 359.0 (2.230)	231.0 (3.555) 280.0 (3.456) 360.0 (2.653)	433.0	428.0	497.0	452.0
1-Butanol	231.0 (3.108) 280.0 (3.080) 357.0 (2.310)	229.0 (3.452) 280.0 (3.356) 359.0 (2.754)	229.0 (3.162) 281.0 (2.997) 361.0 (2.242)	230.0 (3.560) 279.0 (3.476) 360.5 (2.692)	436.0	429.0	499.0	455.0
1-Propanol	231.0 (3.257) 279.0 (3.102) 357.0 (2.413)	231.0 (3.365) 281.5 (3.342) 362.0 (2.292)	229.0 (3.158) 280.0 (2.962) 360.0 (2.238)	232.0 (3.509) 277.0 (3.350) 360.0 (2.672)	437.0	431.0	502.0	446.0
Ethanol	232.0 (3.352) 277.0 (3.132) 356.0 (2.510)	230.0 (3.280) 281.0 (3.262) 362.0 (2.264)	227.0 (3.166) 281.0 (3.013) 360.0 (2.242)	228.0 (3.503) 281.0 (3.470) 361.0 (2.698)	439.0	432.0	503.0	459.0
Acetonitrile	230.0 (3.478) 278.0 (3.078) 357.0 (2.492)	231.0 (3.456) 279.0 (3.142) 361.0 (2.320)	228.0 (3.153) 281.0 (3.018) 358.0 (2.230)	229.0 (3.462) 280.0 (3.466) 359.0 (2.665)	440.0	434.0	505.0	460.0
Solid emission spectra					414.5	407.0	475.0	437.0

[a] UV–vis absorption measured in solution concentration = 1×10^{-5} M.
[b] Photoluminescence measured in solution concentration = 1×10^{-4} M.

high HOMO levels of 5.21–5.41 eV calculated from the oxidation potentials. The LUMO levels were calculated based on the HOMO levels and the lowest energy absorption edges of the UV–vis absorption–emission spectra [33] (Fig. 7). Both the HOMO and LUMO levels of these complexes are summarized in Table 1 and Fig. 8. Substitution of phenyl rings at 1 and 2 position of the imidazole ring increase the energy gap and emits at longer wavelength. Introduction of electron releasing substituents (–OMe) on phenyl ring at 1 position of phenyl ring of the imidazole moiety and electron withdrawing substituent at 2 position of the phenyl ring of

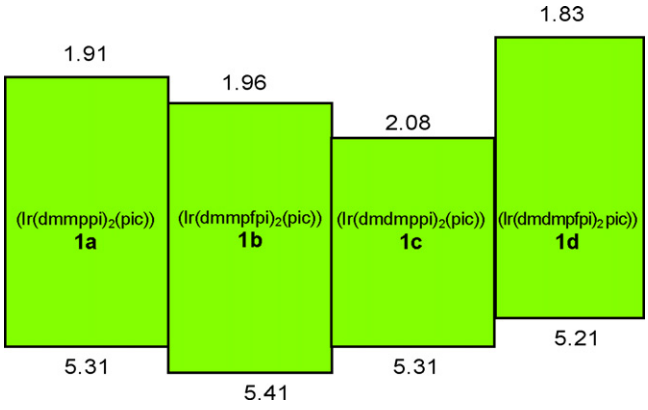

Fig. 8. HOMO–LUMO energy levels.

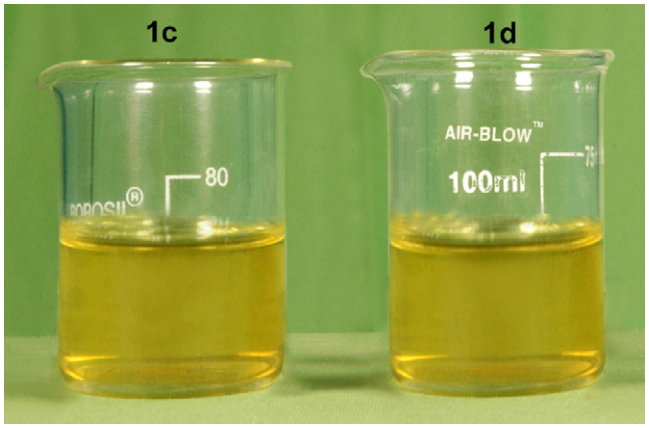

Fig. 9. Solution colour of the photoluminescence for **1c** and **1d**.

the imidazole moiety increases the energy of the HOMO level and decreases the energy of the LUMO level. As the number of electron releasing substituents increased the quantum efficiency increases and emits pure green colour **1c** and **1d** (Fig. 9). It is observed that the phenyl substituted complexes **1a** and **1c** exhibit minimum energy gap (HOMO–LUMO) whereas the fluorophenyl complexes **1b** and **1d** exhibit maximum energy gap. Complex **1c** shows emission at the maximum wavelength whereas complexes **1a** and **1b** exhibit emission at wavelength lower than complex **1c** that can be correlated to the HOMO–LUMO energy gap of the complexes (Table 1). Electroluminescent studies of these complexes are in progress.

4. Conclusion

In conclusion, we have successfully synthesized iridium complexes containing substituted imidazole derivatives as ligands. These complexes exhibit very high HOMO levels compared to pyridine based iridium complexes. In view of the variation of the imidazole ligands that can be synthesized from the method shown in Scheme 1, these complexes are strongly phosphorescent at ambient condition and emits green colour. Further investigation on the effects on luminescent properties depending on tuning the substituent into various positions of the imidazole ligand is currently in progress. Efforts towards the development of blue colour complexes using different substituents are currently underway.

Acknowledgements

Dr. J. Jayabharathi, Reader in Chemistry, Annamalai University is thankful to Department of Science and Technology [No. SR/S1/IC-07/2007] for providing fund to this research work and Prof. C.H. Cheng, Chairman, National Science Council, National Tsing Hua University for her post-doctoral research work.

References

[1] C.W. Tang, S.A. VanSlyke, Organic electroluminescent diodes, Appl. Phys. Lett. 51 (1987) 913–915.
[2] J.H. Burroughes, D.D.C. Bradley, A.R. Brown, R.N. Marks, K. Mackay, R.H. Friend, P.L. Burns, A.B. Holmes, Light-emitting diodes based on conjugated polymers, Nature 347 (1990) 539–541.
[3] M.A. Baldo, M.E. Thompson, S.R. Forrest, Phosphorescent materials for application to organic light emitting devices, Pure Appl. Chem. 71 (1999) 2095–2106.
[4] M.E. Thompson, P.E. Burrows, S.R. Forrest, Electrophosphorescence in organic light emitting diodes, Curr. Opin. Solid State Mater. Sci. 4 (1999) 369–372.
[5] A. Köhler, J.S. Wilson, R.H. Friend, Fluorescence and phosphorescence in organic materials, Adv. Mater. 14 (2002) 701–707.
[6] A.J. Lees, Luminescence properties of organometallic complexes, Chem. Rev. 87 (1987) 711–743.
[7] I.M. Dixon, J.P. Collin, J.P. Sauvage, L. Flamigni, S. Encinas, F. Barigelletti, A family of luminescent coordination compounds: iridium(III) polyimine complexes, Chem. Soc. Rev. 29 (2000) 385–391.
[8] V.W.W. Yam, K.K.W. Lo, Luminescent polynuclear d^{10} metal complexes, Chem. Soc. Rev. 28 (1999) 323–334.
[9] D.S. Tyson, J. Bialecki, F.N. Castellano, Ruthenium(II) complex with a notably long excited state lifetime, Chem. Commun. (2000) 2355–2356.
[10] V.W.W. Yam, S.W.-K. Choi, K.-K. Cheung, Synthesis and design of novel tetranuclear and dinuclear gold(I) phosphine acetylide complexes. First X-ray crystal structures of a tetranuclear ($[Au_4(tppb)(C{\equiv}CPh)_4]$) and a related dinuclear ($[Au_2(dppb)(C{\equiv}CPh)_2]$) complex, Organometallics 15 (1996) 1734–1739.
[11] V.W.W. Yam, K.L. Yu, K.M.C. Wong, K.K. Cheung, Synthesis and structural characterization of a novel luminescent tetranuclear mixed-metal platinum(II)–copper(I) complex, Organometallics 20 (2001) 721–726.
[12] Q.Z. Yang, L.Z. Wu, Z.X. Wu, L.P. Zhang, C.H. Tung, Long-lived emission from platinum(II) terpyridyl acetylide complexes, Inorg. Chem. 41 (2002) 5653–5655.
[13] Y. Ma, H. Zhang, J. Shen, C.M. Che, Electroluminescence from triplet metal-ligand charge-transfer excited state of transition metal complexes, Synth. Met. 94 (1998) 245–248.
[14] Y. Ma, C.M. Che, H.Y. Chao, X. Zhou, W.H. Chan, J. Shen, High luminescence gold(I) and copper(I) complexes with a triplet excited state for use in light-emitting diodes, Adv. Mater. 11 (1999) 852–857.
[15] S. Lamansky, P. Djurovich, D. Murphy, F. Abdel-Razzaq, H.E. Lee, C. Adachi, P.E. Burrows, S.R. Forrest, M.E. Thompson, Highly phosphorescent bis-cyclometalated iridium complexes: synthesis, photophysical characterization and use in organic light emitting diodes, J. Am. Chem. Soc. 123 (2001) 4304–4312.
[16] H.Z. Xie, M.W. Liu, O.Y. Wang, X.H. Zhang, C.S. Lee, L.S. Hung, S.T. Lee, P.F. Teng, H.L. Kwong, H. Zheng, C.M. Che, Reduction of self-quenching effect in organic electrophosphorescence emitting devices via the use of sterically hindered spacers in phosphorescence molecules, Adv. Mater. 13 (2001) 1245–1248.
[17] V.V. Grushin, N. Herron, D.D. LeCloux, W.J. Marshall, V.A. Petrov, Y. Wang, New, efficient electroluminescent materials based on organometallic Ir complexes, Chem. Commun. (2001) 1494–1495.
[18] J. Ostrowski, M.R. Robinson, A.J. Heeger, G.C. Bazan, Amorphous iridium complexes for electrophosphorescent light emitting devices, Chem. Commun. (2002) 784–785.
[19] Y.J. Su, H.L. Huang, C.L. Li, C.H. Chien, Y.T. Tao, P.T. Chou, S. Datta, R.S. Liu, Highly efficient red electrophosphorescent devices based on iridium isoquinoline complexes: remarkable external quantum efficiency over a wide range of current, Adv. Mater. 15 (2003) 884–888.
[20] A.B. Tamayo, B.D. Alleyne, P.I. Djurovich, S. Lamansky, I. Tsyba, N.N. Ho, R. Bau, M.E. Thompson, Synthesis and characterization of facial and meridional tris-cyclometalated iridium(III) complexes, J. Am. Chem. Soc. 125 (2003) 7377–7387.
[21] W. Lu, B.X. Mi, M.C.W. Chan, Z. Hui, N. Zhu, S.T. Lee, C.M. Che, $[(C\hat{N}\hat{N})Pt(C{\equiv}C)_nR]$ [$HC\hat{N}\hat{N}$ = 6-aryl-2,2′-bipyridine, n = 1–4, R = aryl, $SiMe_3$) as a new class of light-emitting materials and their applications in electrophosphorescent devices, Chem. Commun. (2002) 206–207.
[22] B.W. D'Andrade, J. Brooks, V. Adamovich, M.E. Thompson, S.R. Forrest, White light emission using triplet excimers in electrophosphorescent organic light-emitting devices, Adv. Mater. 14 (2002) 1032–1036.
[23] J. Brooks, Y. Babayan, S. Lamansky, P.I. Djurovich, I. Tsyba, R. Bau, M.E. Thompson, Synthesis and characterization of phosphorescent cyclometalated platinum complexes, Inorg. Chem. 41 (2002) 3055–3066.
[24] S. Lamansky, P. Djurovich, D. Murphy, F. Abdel-Razzaq, R. Kwong, I. Tsyba, M. Bortz, B. Mmui, R. Bau, M.E. Thompson, Synthesis and characterization of phosphorescent cyclometalated iridium complexes, Inorg. Chem. 40 (2001) 1704–1711.
[25] M.P. Singh, S. Sasmal, W. Lu, M.N. Chatterjee, Synthetic utility of catalytic Fe(III)/Fe(II) redox cycling towards fused heterocycles: a facile access to substituted benzimidazole, bisbenzimidazole and imidazopyridine derivatives, Synthesis 10 (2000) 1380–1390.
[26] L. Chen, C. Yang, J. Qin, J. Gao, D. Ma, Tuning of emission: synthesis, structure and photophysical properties of imidazole, oxazole and thiazole-based iridium(III) complexes, Inorg. Chim. Acta 359 (2006) 4207–4214.
[27] S. Takizawa, J. Nishida, Phosphorescence color tunable iridium complexes with ligands of 2-phenylimidazo[1,2-*a*]pyridine derivatives, Mol. Cryst. Liq. Cryst. 455 (2006) 381–385.
[28] G. Yoshinobu, H. Noriko, Y. Motoyoshi, Studies on azole compounds. II. Reaction of oxazole N-oxides with phenylisocyanate to give imidazole derivatives, Chem. Pharm. Bull. 18 (1970) 2000–2008.
[29] M. Nonoyama, Benzo(*h*)quinolin-10-yl-N iridium(III) complexes, Bull. Chem. Soc. Jpn. 47 (1974) 767–768.
[30] M.G. Colombo, H.U. Guedel, Synthesis and high-resolution optical spectroscopy of bis[2-(2-thienyl)pyridinato-C3,N′](2,2′-bipyridine)iridium(III), Inorg. Chem. 32 (1993) 3081–3087.
[31] J. DePriest, G.Y. Zheng, N. Goswami, D.M. Eichhorn, C. Woods, D.P. Rillema, Structure, physical and photophysical properties of platinum(II) complexes containing bidentate aromatic and bis(diphenylphosphino)methane as ligands, Inorg. Chem. 39 (2000) 1955–1963.
[32] S. Okada, K. Okinaka, H. Iwawaki, M. Furugori, M. Hashimoto, T. Mukaide, J. Kamatani, S. Igawa, A. Tsuboyama, T. Takiguchi, K. Ueno, Substituent effects of iridium complexes for highly efficient red OLEDs, Dalton Trans. (2005) 1583–1590.
[33] I.R. Laskar, T.-M. Chen, Tuning of wavelengths: synthesis and photophysical studies of iridium complexes and their application in organic light emitting devices, Chem. Mater. 16 (2004) 111–117.
[34] B.-X. Mi, P.-F. Wang, M.-W. Liu, H.-L. Kwong, N.-B. Wong, C.-S. Lee, S.-T. Lee, Thermally stable hole-transporting material for organic light-emitting diode: an isoindole derivative, Chem. Mater. 15 (2003) 3148–3151.
[35] S. Ranjan, S.Y. Lin, K.C. Hwang, Y. Chi, W.L. Ching, C.S. Liu, Y.T. Tao, C.H. Chien, S.M. Peng, G.H. Lee, Realizing green phosphorescent light-emitting materials from rhenium(I) pyrazolato diimine complexes, Inorg. Chem. 42 (2003) 1248–1255.